

Markus Berndt · Konstantin Lipnikov
Mikhail Shashkov · Mary F. Wheeler
Ivan Yotov

A mortar mimetic finite difference method on non-matching grids

Received: 30 July 2004 / Revised: 28 April 2005 / Published online: 22 September 2005
© Springer-Verlag 2005

Abstract We consider mimetic finite difference approximations to second order elliptic problems on non-matching multiblock grids. Mortar finite elements are employed on the non-matching interfaces to impose weak flux continuity. Optimal convergence and, in certain cases, superconvergence is established for both the scalar variable and its flux. The theory is confirmed by computational results.

Mathematics Subject Classification (2000): 65N06 · 65N12 · 65N15 · 65N22 · 65N30

1 Introduction

Mortar methods for finite element discretizations have been popular since they provide a natural framework for domain decomposition. It is often desirable to divide the computational domain into non-overlapping blocks, where grids are defined

M. Berndt (✉) · K. Lipnikov · M. Shashkov

Los Alamos National Laboratory, Mail Stop B284, Los Alamos, NM 87545, USA

E-mail: {berndt,lipnikov,shashkov}@lanl.gov.

Supported by the US Department of Energy, under contract W-7405-ENG-36. LA-UR-04-4740.

M. F. Wheeler

Institute for Computational Engineering and Sciences (ICES), Department of Aerospace Engineering and Engineering Mechanics, and Department of Petroleum and Geosystems Engineering, The University of Texas at Austin, Austin, TX 78712, USA

E-mail: mfw@ices.utexas.edu.

Partially supported by NSF grants EIA 0121523 and DMS 0411413, by NPACI grant UCSD 10181410, and by DOE grant DE-FGO2-04ER25617.

I. Yotov

Department of Mathematics, 301 Thackeray Hall, University of Pittsburgh, Pittsburgh, PA 15260, USA

E-mail: yotov@math.pitt.edu.

Partially supported by NSF grants DMS 0107389, DMS 0112239 and DMS 0411694 and by DOE grant DE-FGO2-04ER25618.

independently on each of these blocks. The geometry of the problem, discontinuities in the material properties, or features in the solution may provide a natural decomposition of the problem domain into multiple such blocks. In this paper we develop a mortar method in the framework of mimetic finite difference (MFD) methods. This method has the advantages of a standard MFD method. It employs discrete operators that preserve locally certain critical properties of the original continuum differential operators, such as conservation laws, solution symmetries, and fundamental identities of vector calculus. In addition to that, it also inherits the benefits that stem from the mortar framework.

We develop the method for second order linear elliptic equations. Introducing a flux variable, we solve for a scalar function p and a vector function \mathbf{u} satisfying

$$\mathbf{u} = -K \nabla p \quad \text{in } \Omega, \quad (1.1)$$

$$\nabla \cdot \mathbf{u} = b \quad \text{in } \Omega, \quad (1.2)$$

$$p = g \quad \text{on } \partial\Omega, \quad (1.3)$$

where $\Omega \subset \mathbb{R}^{dim}$, $dim = 2$ or 3 , is a multiblock domain with a Lipschitz continuous boundary, and K is a symmetric, uniformly positive definite tensor with $L^\infty(\Omega)$ components. The Dirichlet boundary conditions are considered merely for simplicity. In porous media applications the system (1.1)–(1.3) models single phase Darcy flow, where p is the pressure, \mathbf{u} is the velocity, and K represents the rock permeability divided by the fluid viscosity.

The *mimetic* technique has been successfully employed in a number of science and engineering applications, including diffusion [26, 16, 21], continuum mechanics [20], and gas dynamics [9]. MFD methods work well for problems with rough coefficients and general grids, including unstructured three-dimensional meshes comprised of hexahedra, tetrahedra, and any cell type that has three faces intersecting at each vertex [15]. The method has also been extended to locally refined meshes with hanging nodes [19].

A connection between the MFD method and the MFE method with Raviart-Thomas finite elements was established in [5]. This was achieved by showing that the scalar product in the velocity space proposed in [16] for MFD methods can be viewed as a quadrature rule in the context of MFE methods. In [6], superconvergence for the normal velocities in MFD methods on h^2 -uniform quadrilateral meshes was established.

Mixed finite element (MFE) discretizations on quadrilateral meshes [27, 28, 2, 12] are based on the Piola transformation [27, 7], which preserves continuity of the normal component of the velocity across mesh edges, but results in the necessity to integrate rational functions over quadrilaterals. This is further complicated in the case of a full or non-constant diffusion tensor. The results in [5] provide an efficient numerical quadrature with a minimal number of points, also allowing for the extension of MFE methods to general polygons and polyhedrons.

The mortar MFE method has been studied, for example, in [31, 1] (see also [4, 3, 30] for seminal work on mortar couplings for Galerkin finite element discretizations). In these methods, the domain is divided into nonoverlapping subdomain blocks, and each of these subdomain blocks is discretized on a locally constructed mesh. As a result, the subdomain grids do not match at inter block boundaries. To solve this problem, Lagrange multiplier pressures are introduced at the inter block boundaries. This Lagrange multiplier space is called the mortar finite element

space. It was shown in [1] that the mortar MFE method is optimally convergent, if the boundary space has one order higher approximability than the normal trace of the velocity space. The multiblock structure of the mortar MFE systems allows for scalable parallel domain decomposition solvers and preconditioners, which maximize data and computation locality, to be developed and applied [1, 29]. Mortar techniques are also very suitable for multiphysics applications [23].

In this paper, we employ mortar techniques to extend the MFD method to the case of non-matching multiblock grids. Discrete interface continuity conditions are derived in the MFD framework, based on a piecewise linear mortar finite element space. We exploit the relation between MFD and MFE methods to give a variational formulation of the mortar MFD method and study its convergence properties. We establish optimal convergence for both the pressure and the velocity on quadrilateral, triangular, and tetrahedral grids. We also prove superconvergence for the pressure at the cell centers and, in the case of h^2 -uniform quadrilateral grids, superconvergence for the normal velocities at the midpoints of the edges. The results here can be viewed as extensions of the MFD convergence results of [5] and velocity superconvergence results of [6] to the case of non-matching multiblock grids. We also note that, to the best of our knowledge, no previous pressure superconvergence results for the MFD methods have been reported.

The outline of the paper is as follows. In Section 2, we describe the mortar MFD method. In particular, we extend the MFD method to the case of non-overlapping subdomain blocks with non-matching grids by defining appropriate discrete interface conditions. In Section 3, the mortar MFE method is described, and in Section 4 it is related to the mortar MFD method. In Sections 5 and 6, we give error estimates for the velocity and the pressure, respectively. In Section 7, we confirm the theory with numerical experiments, and in Section 8, we make concluding remarks.

2 The mortar mimetic finite difference method

The fundamental idea in a mortar method is to decompose the computational domain into non-overlapping subdomains. To that end, we assume that Ω can be decomposed into non-overlapping polygonal subdomain blocks Ω_i ,

$$\bar{\Omega} = \bigcup_{i=1}^n \bar{\Omega}_i.$$

Denote by $\Gamma_{i,j} = \partial\Omega_i \cap \partial\Omega_j$ the interior block interfaces. Let

$$\Gamma = \bigcup_{i,j=1}^n \Gamma_{i,j}, \quad \text{and} \quad \Gamma_i = \partial\Omega_i \cap \Gamma = \partial\Omega_i \setminus \partial\Omega.$$

Let $\mathcal{T}_{h,i}$ be a conforming, *shape-regular*, quasi-uniform partition of Ω_i , $1 \leq i \leq n$ [10], allowing for $\mathcal{T}_{h,i}$ and $\mathcal{T}_{h,j}$ to be non-matching on $\Gamma_{i,j}$. We will consider simplicial elements in two and three dimensions as well as convex quadrilateral elements in two dimensions. Let $\mathcal{E}_{h,i,j}$ be the trace of mesh $\mathcal{T}_{h,i}$ on the interface $\Gamma_{i,j}$ and let $\mathcal{E}_{h,i}$ be the trace of $\mathcal{T}_{h,i}$ on $\partial\Omega_i$. In our derivation, we use a quasi-uniform partition of $\Gamma_{i,j}$ that is not necessarily the trace of $\mathcal{T}_{h,i}$ on the interface $\Gamma_{i,j}$. We denote this partition by $\tilde{\mathcal{E}}_{h,i,j}$, and postulate that $\tilde{\mathcal{E}}_{h,i,j} \equiv \tilde{\mathcal{E}}_{h,j,i}$. This partition will

be used to impose interface matching conditions via mortar finite elements. Finally, we denote by

$$\mathcal{T}_h = \bigcup_{i=1}^n \mathcal{T}_{h,i}.$$

the partition of the multiblock domain Ω .

2.1 Mimetic finite difference subdomain discretization

In this section, we derive two mutually adjoint discrete operators with respect to certain scalar products in discrete velocity and pressure spaces. These discrete operators form the basis for the mimetic finite difference (MFD) method. To begin, we now consider only one subdomain Ω_i and the spaces $X_i = L^2(\Omega_i)$ of velocities and $Q_i = H^1(\Omega_i)$ of pressures. These spaces are equipped with the scalar products

$$(\mathbf{u}, \mathbf{v})_{X_i} = \int_{\Omega_i} K^{-1} \mathbf{u} \cdot \mathbf{v} \, dx \quad \text{and} \quad (p, q)_{Q_i} = \int_{\Omega_i} pq \, dx + \oint_{\partial\Omega_i} pq \, ds.$$

On these two spaces, we introduce flux operator $\mathcal{G} : Q_i \rightarrow X_i$ and extended divergence operator $\mathcal{D} : X_i \rightarrow Q_i$ by

$$\mathcal{G}p = -K\nabla p, \quad \mathcal{D}\mathbf{u} = \begin{cases} \nabla \cdot \mathbf{u} & \text{on } \Omega_i, \\ -\mathbf{u} \cdot \mathbf{n}_i & \text{on } \partial\Omega_i, \end{cases}$$

where \mathbf{n}_i is the outer unit normal to $\partial\Omega_i$.

The Gauss–Green formula can now be stated using this notation as

$$(\mathbf{u}, \mathcal{G}p)_{X_i} = (p, \mathcal{D}\mathbf{u})_{Q_i} \quad \forall p \in Q_i, \quad \mathbf{u} \in X_i.$$

This implies that the flux and extended divergence are adjoint operators, in other words $\mathcal{G} = \mathcal{D}^*$. For the sake of simplicity, we omit subscript ‘ i ’ whenever this does not result in ambiguity. Unless we specifically state it, the following applies to both 2D and 3D, and we will use the term face in both cases, such that we refer to an edge in 2D as a face.

The *first* step in the derivation of the MFD method is to specify discrete degrees of freedom for the primary variables, pressure and velocity. We choose the discrete pressure unknowns to be located at the geometric centers of mesh elements of $\mathcal{T}_{h,i}$. Additional discrete pressure unknowns are located at centers of boundary faces of $\mathcal{E}_{h,i}$ (see Fig. 1). We choose discrete unknowns that represent the normal component of the velocity to be located at midpoints of mesh faces of $\mathcal{T}_{h,i}$. In other words, this face-based unknown is a scalar and represents the orthogonal projection of a velocity vector onto the unit vector normal to the mesh face. The direction of the normal vector is *a priori* fixed. We also assume that normal vectors to boundary edges are outward vectors (see Fig. 1).

In the *second* step of the MFD method, we equip the spaces of discrete pressures and normal velocities with scalar products. Here, we denote the vector space of discrete pressures by Q_i^d . Denote by E and f an element and a face in the partition

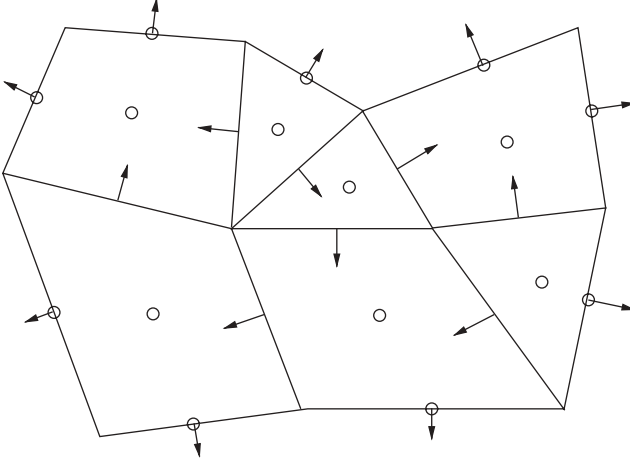


Fig. 1 Location of pressure unknowns (marked by bullets) and velocity unknowns (marked by arrows)

$\mathcal{T}_{h,i}$, respectively, and by p_E and p_f the pressure components associated with E and f , respectively. Then we define the scalar product on the vector space \mathcal{Q}_i^d as

$$[\vec{p}, \vec{q}]_{\mathcal{Q}_i^d} = \sum_{E \in \mathcal{T}_{h,i}} |E| p_E q_E + \sum_{f \in \mathcal{E}_{h,i}} |f| p_f q_f, \quad \forall \vec{p}, \vec{q} \in \mathcal{Q}_i^d, \quad (2.1)$$

where, $|E|$ denotes the volume (or, in 2D, the area) of element E and $|f|$ denotes the area (or, in 2D, length) of face f . Let $\mathcal{Q}_i^{d,0}$ be the vector space of only cell-based unknowns. The scalar product on $\mathcal{Q}_i^{d,0}$ is defined as only the first sum in (2.1).

We denote the vector space of face-centered normal velocities by X_i^d and define the scalar product on X_i^d as

$$[\vec{u}, \vec{v}]_{X_i^d} = \sum_{E \in \mathcal{T}_{h,i}} [\vec{u}, \vec{v}]_{X_i^d, E}, \quad (2.2)$$

where $[\vec{u}, \vec{v}]_{X_i^d, E}$ is a scalar product over an element E , involving only normal velocity components on element faces. To complete the second step, we now define this element scalar product.

We note that a velocity vector in \mathbb{R}^{dim} can be recovered from dim orthogonal projections on any dim linearly independent vectors. For example, for a convex non-degenerate cell in \mathbb{R}^3 , any triplet of normal vectors to faces with a common point satisfy the above requirement. These orthogonal projections are chosen as degrees of freedom. The recovered velocities are used to define scalar product (2.2). To illustrate this recovery process, we consider two examples. Let E be a convex polygon with s edges ($s = 3$ for a triangle and $s = 4$ for a quadrilateral). As illustrated in Fig. 2, four recovered velocity vectors can be associated with the four vertices of a quadrilateral. For example, velocity \mathbf{v}_1 is recovered from its projections onto the normal vectors \mathbf{n}_1 and \mathbf{n}_2 . In the general case, we denote by $\mathbf{v}(\mathbf{r}_k)$ the velocity recovered at the k -th vertex \mathbf{r}_k of E , $k = 1, \dots, s$.

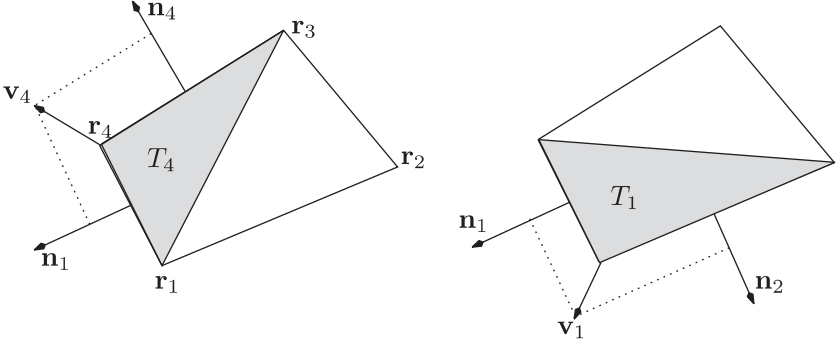


Fig. 2 Recovered vectors $\mathbf{v}_1, \mathbf{v}_4$ and triangles T_1, T_4

In this paper, we consider two cell-based scalar products in 2D. The first one is given by

$$[\vec{u}, \vec{v}]_{X_i^d, E} = \frac{1}{\alpha_E} \sum_{k=1}^s |T_k| K^{-1}(\mathbf{r}_k) \mathbf{u}(\mathbf{r}_k) \cdot \mathbf{v}(\mathbf{r}_k), \quad \alpha_E = \frac{1}{|E|} \sum_{k=1}^s |T_k|, \quad (2.3)$$

where $|T_k|$ is the area of the triangle formed by the two edges sharing the k -th vertex. See, for example, the shaded triangles T_1 and T_4 in Fig. 2. Note that $\alpha_E = 3$ for triangles and $\alpha_E = 2$ for quadrilaterals. The second cell-based scalar product requires only one evaluation of the tensor K and is given by

$$[\vec{u}, \vec{v}]_{X_i^d, E} = \frac{1}{\alpha_E} \sum_{k=1}^s |T_k| K_E^{-1} \mathbf{u}(\mathbf{r}_k) \cdot \mathbf{v}(\mathbf{r}_k) \quad (2.4)$$

where K_E is the value of tensor K at the center of gravity of E .

Note that both (2.2), (2.3) and (2.2), (2.4) are indeed scalar products on X_i^d , since K is a uniformly bounded, symmetric and positive definite tensor, and there are two positive constants c_1 and c_2 independent of h such that

$$c_1 |E| \sum_{f \subset \partial E} v_f^2 \leq [\vec{v}, \vec{v}]_{X_i^d, E} \leq c_2 |E| \sum_{f \subset \partial E} v_f^2 \quad (2.5)$$

where v_f denotes the velocity component associated with face f .

In the 3D case, we only allow E to be a tetrahedron. Since each vertex of E is shared by exactly three faces, we can uniquely recover velocity vectors at the vertices of E . The scalar product over E is given either by (2.3) or by (2.4) with $s = 4$. Since in the case of tetrahedron $T_k = E$, we have $\alpha_E = 4$.

The *third* step of the MFD method is to derive a discrete approximation to the divergence operator, DIV^d , which we shall refer to as the *prime* operator. We use the divergence theorem on element E to define this discrete divergence operator as

$$(DIV^d \vec{u}) \Big|_E \equiv \frac{1}{|E|} \sum_{f \subset \partial E} u_f |f| \quad (2.6)$$

Formula (2.6) assumes an external orientation of normal vectors. If the vector normal to face f points into the element (see, e.g. Fig. 1), u_f must be replaced by $-u_f$. The extended discrete divergence operator, $\mathcal{D}^d : X_i^d \rightarrow Q_i^d$, is given by

$$\mathcal{D}^d \vec{u} = \begin{cases} (\text{DIV}^d \vec{u})|_E & \forall E \in \mathcal{T}_{h,i}, \\ -u_f & \forall f \in \mathcal{E}_{h,i}. \end{cases} \quad (2.7)$$

In the *fourth step* of the MFD method, a discrete flux operator \mathcal{G}^d that is adjoint to the discrete extended divergence operator \mathcal{D}^d with respect to the scalar products (2.1) and (2.2) is derived, i.e.

$$\left[\mathcal{D}^d \vec{u}, \vec{p} \right]_{Q_i^d} \equiv \left[\vec{u}, \mathcal{G}^d \vec{p} \right]_{X_i^d} \quad \forall \vec{u} \in X_i^d, \vec{p} \in Q_i^d. \quad (2.8)$$

We will refer to (2.8) as discrete Green's formula. See [5] for the explicit form of the operator \mathcal{G}^d . Now, the MFD method for subdomain Ω_i may be summarized as follows:

$$\begin{aligned} \vec{u} &= \mathcal{G}^d \vec{p}, \\ \text{DIV}^d \vec{u} &= \vec{b}, \end{aligned} \quad (2.9)$$

where \vec{b} is in Q_i^d . The entries of \vec{b} are integral averages of right-hand side b in (1.2) over the elements of $\mathcal{T}_{h,i}$.

The MFD method (2.9) is presented using notation that is well established in the finite difference and finite volume communities. In Section 4, we rewrite it in a variational form (4.2) to relate mortar MFD and mortar MFE methods.

2.2 Interface conditions between subdomain blocks

To derive the mortar MFD discretization on Ω , we must impose continuity conditions at interfaces $\Gamma_{i,j}$ between subdomains Ω_i and Ω_j and boundary conditions on Γ . Hereafter, we will use subscript 'i' for vectors and operators satisfying equation (2.9) on subdomain Ω_i .

We recall that the solution of (1.1)–(1.3) satisfies continuity conditions at interfaces $\Gamma_{i,j}$. In particular, the pressure and the normal flux are both continuous almost everywhere across $\Gamma_{i,j}$. We will refer to these conditions as interface continuity conditions. In order to impose these conditions discretely on non-matching grids, we introduce the intermediate vector space $\Lambda_{i,j}^d \equiv \Lambda_{j,i}^d$ that is associated with the interface partition $\tilde{\mathcal{E}}_{h,i,j}$. We will make precise the definition of $\Lambda_{i,j}^d$ later in Section 4, where it will be related to a mortar space in a mixed finite element method.

Denote by $Q_{i,j}^d$ the vector space of pressure unknowns associated with the faces of partition $\mathcal{E}_{h,i,j}$. We define the scalar product in $Q_{i,j}^d$ to be

$$\left[\vec{p}_{i,j}, \vec{q}_{i,j} \right]_{Q_{i,j}^d} = \sum_{f \subset \mathcal{E}_{h,i,j}} |f| p_{i,j,f} q_{i,j,f}$$

where $p_{i,j,f}$ (resp., $q_{i,j,f}$) is the component of vector $\vec{p}_{i,j}$ (resp., $\vec{q}_{i,j}$) associated with face f .

Similarly, we define the vector space $X_{i,j}^d$ of velocity unknowns associated with the faces of partition $\mathcal{E}_{h,i,j}$. We choose $X_{i,j}^d$ to be isometric to $Q_{i,j}^d$, i.e.

$$[\vec{u}_{i,j}, \vec{v}_{i,j}]_{X_{i,j}^d} = [\vec{u}_{i,j}, \vec{v}_{i,j}]_{Q_{i,j}^d}.$$

Finally, let $R_{i,j} : \Lambda_{i,j}^d \rightarrow Q_{i,j}^d$ be a linear projection operator that is exact for constant vectors. We will make precise the definition of $R_{i,j}$ later in Section 4, where it will be related to the orthogonal projector from the mortar finite element space to the space of piecewise constant functions.

Discrete interface continuity conditions are derived from two requirements. First, we require *mass conservation* across $\tilde{\mathcal{E}}_{h,i,j}$, i.e.

$$[\vec{u}_{i,j}, R_{i,j}\vec{\mu}]_{X_{i,j}^d} = -[\vec{u}_{j,i}, R_{j,i}\vec{\mu}]_{X_{j,i}^d} \quad \forall \vec{\mu} \in \Lambda_{i,j}^d. \quad (2.10)$$

Let $F_{i,j}$ be the diagonal matrix with entries that are the areas of faces of $\mathcal{E}_{h,i,j}$. It is not difficult to see that mass conservation (2.10) implies the interface condition

$$R_{i,j}^T F_{i,j} \vec{u}_{i,j} = -R_{j,i}^T F_{j,i} \vec{u}_{j,i}. \quad (2.11)$$

Second, we require that *the discrete Green's formula (2.8) holds on $\bar{\Omega}_i \cup \bar{\Omega}_j$* . It is easy to see that this holds if the sum of the discrete Green's formulas for Ω_i and Ω_j cancels the boundary terms associated with the common interface, i.e.

$$[\vec{p}_{i,j}, \vec{u}_{i,j}]_{Q_{i,j}^d} = -[\vec{p}_{j,i}, \vec{u}_{j,i}]_{Q_{j,i}^d}.$$

Hence, a sufficient condition for the validity of the discrete Green's formula on $\Omega_i \cup \Omega_j$ is

$$\exists \vec{\lambda} \in \Lambda_{i,j}^d : \quad \vec{p}_{i,j} = R_{i,j}\vec{\lambda} \quad \text{and} \quad \vec{p}_{j,i} = R_{j,i}\vec{\lambda}. \quad (2.12)$$

In the general case, $\vec{\lambda}$ is considered as an additional unknown.

Remark 2.1 Locally refined meshes can be viewed as non-matching meshes. In this special case, vector $\vec{\lambda}$ can be eliminated from (2.12). In Section 7, we derive simple formulas for the discrete interface continuity conditions on such meshes.

The mortar MFD method for (1.1)–(1.3) is defined by combining the system of subdomain equations (2.9) with the interface continuity conditions (2.11) and (2.12) and the boundary conditions

$$p_f = g_f \quad \forall f \subset \partial\Omega, \quad (2.13)$$

where g_f is the integral average of g over face f .

3 The mortar mixed finite element method

In this section we briefly recall the mortar mixed finite element method introduced in [31, 1], which will later be related to the mortar MFD method that was introduced in the previous section. We follow the standard notations for norms, semi-norms and scalar products. A weak solution of (1.1)–(1.3) is a pair $(\mathbf{u}, p) \in H(\operatorname{div}; \Omega) \times L^2(\Omega)$, such that

$$(K^{-1}\mathbf{u}, \mathbf{v}) = (p, \nabla \cdot \mathbf{v}) - \langle g, \mathbf{v} \cdot \mathbf{n} \rangle_{\partial\Omega} \quad \forall \mathbf{v} \in H(\operatorname{div}; \Omega), \quad (3.1)$$

$$(\nabla \cdot \mathbf{u}, w) = (b, w) \quad \forall w \in L^2(\Omega). \quad (3.2)$$

It is well known (see, e.g., [7, 25]) that (3.1)–(3.2) has a unique solution. The multi-domain formulation of (3.1)–(3.2) is based on the spaces

$$\begin{aligned} \mathbf{V}_i &= H(\operatorname{div}; \Omega_i), & \mathbf{V} &= \bigoplus_{i=1}^n \mathbf{V}_i, \\ W_i &= L^2(\Omega_i), & W &= \bigoplus_{i=1}^n W_i = L^2(\Omega). \end{aligned}$$

If the solution (\mathbf{u}, p) of (3.1)–(3.2) belongs to $H(\operatorname{div}; \Omega) \times H^1(\Omega)$, it is easy to see [7, pp. 91–92] that it satisfies, for $1 \leq i \leq n$,

$$(K^{-1}\mathbf{u}, \mathbf{v})_{\Omega_i} = (p, \nabla \cdot \mathbf{v})_{\Omega_i} - \langle p, \mathbf{v} \cdot \mathbf{n}_i \rangle_{\Gamma_i} - \langle g, \mathbf{v} \cdot \mathbf{n}_i \rangle_{\partial\Omega_i \setminus \Gamma} \quad \forall \mathbf{v} \in \mathbf{V}_i, \quad (3.3)$$

$$(\nabla \cdot \mathbf{u}, w)_{\Omega_i} = (b, w)_{\Omega_i} \quad \forall w \in W_i. \quad (3.4)$$

The mortar mixed finite element method discretizes (3.3)–(3.4), coupled with a mortar-based discretization of the interface conditions. Next, we present the definition of the mixed finite element spaces. We describe the two-dimensional elements: quadrilaterals and triangles. The finite element spaces for a tetrahedral element are constructed similarly to the finite element spaces for a triangular element.

For any element $E \in \mathcal{T}_h$, there exists a bijection mapping $F_E: \hat{E} \rightarrow E$, where \hat{E} is the reference element. For example, in the case of convex quadrilaterals, \hat{E} is the unit square with vertices $\hat{\mathbf{r}}_1 = (0, 0)^T$, $\hat{\mathbf{r}}_2 = (1, 0)^T$, $\hat{\mathbf{r}}_3 = (1, 1)^T$ and $\hat{\mathbf{r}}_4 = (0, 1)^T$. Denote by $\mathbf{r}_i = (x_i, y_i)^T$, $i = 1, 2, 3, 4$, the four corresponding vertices of an element E as shown in Fig. 3. Then, F_E is the bilinear mapping given by

$$F_E(\hat{\mathbf{r}}) = \mathbf{r}_1(1 - \hat{x})(1 - \hat{y}) + \mathbf{r}_2\hat{x}(1 - \hat{y}) + \mathbf{r}_3\hat{x}\hat{y} + \mathbf{r}_4(1 - \hat{x})\hat{y}.$$

Note that the Jacobi matrix DF_E and its Jacobian J_E are linear functions of \hat{x} and \hat{y} . Indeed, straightforward computations yield

$$DF_E = [(1 - \hat{y})\mathbf{r}_{21} + \hat{y}\mathbf{r}_{34}, (1 - \hat{x})\mathbf{r}_{41} + \hat{x}\mathbf{r}_{32}],$$

and

$$J_E = 2|T_1| + 2(|T_2| - |T_1|)\hat{x} + 2(|T_4| - |T_1|)\hat{y}, \quad (3.5)$$

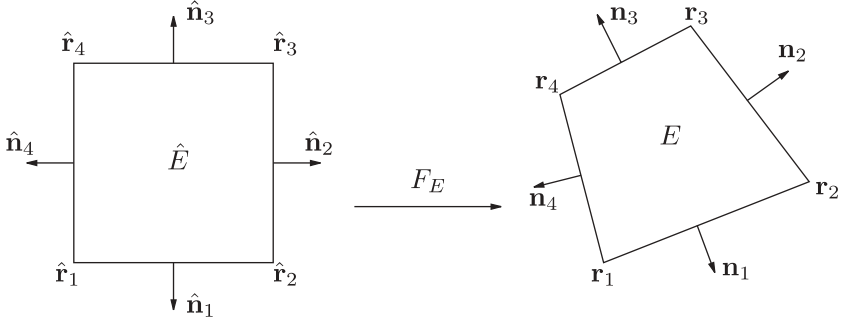


Fig. 3 Bilinear mapping and orientation of normal vectors

where $\mathbf{r}_{ij} = \mathbf{r}_i - \mathbf{r}_j$ and triangles T_k , $k = 1, 2, 3, 4$, are defined in (2.3). Since E is convex, the Jacobian J_E is uniformly positive, i.e. $J_E(\hat{x}, \hat{y}) > 0$. We denote the inverse mapping by F_E^{-1} and its Jacobian by $J_{F_E^{-1}}$.

In the case of triangles, \hat{E} is the reference right triangle with vertices $\hat{\mathbf{r}}_1 = (0, 0)^T$, $\hat{\mathbf{r}}_2 = (1, 0)^T$, and $\hat{\mathbf{r}}_3 = (0, 1)^T$. Let \mathbf{r}_1 , \mathbf{r}_2 , and \mathbf{r}_3 be the corresponding vertices of E , oriented in a counter clockwise direction. The linear mapping for triangles has the form

$$F_E(\hat{\mathbf{r}}) = \mathbf{r}_1(1 - \hat{x} - \hat{y}) + \mathbf{r}_2\hat{x} + \mathbf{r}_3\hat{y}, \quad (3.6)$$

with respective Jacobi matrix and Jacobian

$$DF_E = [\mathbf{r}_{21}, \mathbf{r}_{31}]^T \quad \text{and} \quad J_E = 2|E|. \quad (3.7)$$

Note that in this case the mapping is affine and the Jacobi matrix and its Jacobian are constants.

We denote the lowest order Raviart-Thomas-Nedelec (RTN) mixed finite element spaces [27, 24, 22] by

$$\mathbf{V}_{h,i} \times W_{h,i} \subset \mathbf{V}_i \times W_i$$

These spaces are initially defined on the reference element. For example, if \hat{E} is the unit square, the spaces are

$$\hat{\mathbf{V}}(\hat{E}) = P_{1,0}(\hat{E}) \times P_{0,1}(\hat{E}) \quad \text{and} \quad \hat{W}(\hat{E}) = P_0(\hat{E}),$$

where $P_{1,0}$ (or $P_{0,1}$) denotes the space of polynomials linear in the \hat{x} (or \hat{y}) variable and constant in the other variable, and P_0 denotes the space of constant functions. In the case when \hat{E} is the unit triangle, the spaces on this reference element are

$$\hat{\mathbf{V}}(\hat{E}) = P_0(\hat{E}) \times P_0(\hat{E}) + P_0(\hat{E})\hat{\mathbf{x}} \quad \text{and} \quad \hat{W}(\hat{E}) = P_0(\hat{E}).$$

The velocity space on any element E is defined via the Piola transformation

$$\frac{1}{J_E} DF_E : (L_2(\hat{E}))^{dim} \rightarrow (L_2(E))^{dim} \quad \forall E \in \mathcal{T}_h.$$

The RTN_0 spaces on $\mathcal{T}_{h,i}$ are given by

$$\begin{aligned} \mathbf{V}_{h,i} &= \{\mathbf{v} \in \mathbf{V}_i : \mathbf{v}|_E = J_E^{-1} DF_E \hat{\mathbf{v}} \circ F_E^{-1}, \hat{\mathbf{v}} \in \hat{\mathbf{V}}(\hat{E}) \quad \forall E \in \mathcal{T}_{h,i}\}, \\ W_{h,i} &= \{w \in W_i : w|_E = \hat{w} \circ F_E^{-1}, \hat{w} \in \hat{W}(\hat{E}) \quad \forall E \in \mathcal{T}_{h,i}\}. \end{aligned} \quad (3.8)$$

The following two properties of the Piola transformation will be useful in the analysis. For any $\hat{\mathbf{v}} \in \hat{\mathbf{V}}(\hat{E})$ and the related $\mathbf{v} = J_E^{-1} DF_E \hat{\mathbf{v}} \circ F_E^{-1}$, we have

$$\int_E \nabla \cdot \mathbf{v} \, d\mathbf{x} = \int_{\hat{E}} \hat{\nabla} \cdot \hat{\mathbf{v}} \, d\hat{\mathbf{x}} \quad \text{and} \quad \int_f \mathbf{v} \cdot \mathbf{n}_f \, ds = \int_{\hat{f}} \hat{\mathbf{v}} \cdot \hat{\mathbf{n}}_{\hat{f}} \, d\hat{s}, \quad (3.9)$$

where f is any face of E and \mathbf{n}_f and $\hat{\mathbf{n}}_{\hat{f}}$ are the unit normal vectors to f and \hat{f} , respectively.

The quasi-uniform partition $\tilde{\mathcal{E}}_{h,i,j}$ of $\Gamma_{i,j}$ introduced above is referred to as the mortar interface mesh. Denote by $\Lambda_{h,i,j} \subset L^2(\Gamma_{i,j})$ the mortar space on $\Gamma_{i,j}$, containing either the continuous or discontinuous piecewise linear polynomials on $\tilde{\mathcal{E}}_{h,i,j}$. Let

$$\mathbf{V}_h = \bigoplus_{i=1}^n \mathbf{V}_{h,i}, \quad W_h = \bigoplus_{i=1}^n W_{h,i}, \quad \Lambda_h = \bigoplus_{1 \leq i < j \leq n} \Lambda_{h,i,j}.$$

Although normal components of vectors in \mathbf{V}_h are continuous between elements within each block Ω_i , there is no such restriction across Γ . The space Λ_h is called the mortar finite element space on Γ . In the following we treat any function $\mu \in \Lambda_h$ as extended by zero on $\partial\Omega$. An additional assumption on the space Λ_h , and hence $\tilde{\mathcal{E}}_{h,i,j}$, will be made below in (4.7) and (5.13). We remark that $\tilde{\mathcal{E}}_{h,i,j}$ need not be conforming if a discontinuous space is used.

In the mortar mixed finite element approximation of (3.1)–(3.2), we seek $\mathbf{u}_h \in \mathbf{V}_h$, $p_h \in W_h$, $\lambda_h \in \Lambda_h$ such that, for $1 \leq i \leq n$,

$$(K^{-1} \mathbf{u}_h, \mathbf{v})_{\Omega_i} = (p_h, \nabla \cdot \mathbf{v})_{\Omega_i} - \langle \lambda_h, \mathbf{v} \cdot \mathbf{n}_i \rangle_{\Gamma_i} - \langle g, \mathbf{v} \cdot \mathbf{n}_i \rangle_{\partial\Omega_i \setminus \Gamma} \quad \forall \mathbf{v} \in \mathbf{V}_{h,i}, \quad (3.10)$$

$$(\nabla \cdot \mathbf{u}_h, w)_{\Omega_i} = (b, w)_{\Omega_i} \quad \forall w \in W_{h,i}, \quad (3.11)$$

$$\sum_{i=1}^n \langle \mathbf{u}_h \cdot \mathbf{n}_i, \mu \rangle_{\Gamma_i} = 0 \quad \forall \mu \in \Lambda_h. \quad (3.12)$$

Remark 3.1 The above method imposes continuity of the pressure by approximating the pressure on the interfaces by a single-valued mortar function λ_h , while continuity of the normal flux is imposed weakly in (3.12) with respect to Lagrange multipliers in the mortar space.

4 Relating mortar MFD and mortar MFE methods

The basic tool for the error analysis of the mortar MFD method is based on establishing connections with the mortar mixed finite element (MFE) method (3.10)–(3.12). We begin by establishing an isomorphism between finite difference and finite element spaces.

The degrees of freedom of $\mathbf{V}_{h,i}$ are associated with mesh faces. Therefore, the space $\mathbf{V}_{h,i}$ is isomorphic to the vector space X_i^d . Similarly, the degrees of freedom of the finite element space $W_{h,i}$ are associated with cell centers and the space is isometric to the vector space $Q_i^{d,0}$ equipped with the norm induced by its scalar product defined in Section 2.1 (see also [5]). By the same arguments, the vector space $X_{i,j}^d$ is isometric to the finite element space $\mathbf{V}_{h,i} \cdot \mathbf{n}_i|_{\Gamma_{i,j}}$.

Finally, we choose $\Lambda_{i,j}^d$ to be isomorphic to the finite element space $\Lambda_{h,i,j}$. In particular, degrees of freedom of $\Lambda_{i,j}^d$ are the values of the pressure at vertices of partition $\tilde{\mathcal{E}}_{h,i,j}$. In the case of discontinuous mortars, each vertex may be associated with multiple degrees of freedom. The projector $R_{i,j}$ is implicitly defined by

$$[R_{i,j}\tilde{\mu}_{i,j}, \tilde{q}_{i,j}]_{Q_{i,j}^d} = \langle \mu_{h,i,j}, q_{h,i,j} \rangle_{\Gamma_{i,j}} \quad \forall \tilde{\mu}_{i,j} \in \Lambda_{i,j}^d, \tilde{q}_{i,j} \in Q_{i,j}^d, \quad (4.1)$$

where $\mu_{h,i,j} \in \Lambda_{h,i,j}$ and $q_{h,i,j} \in \mathbf{V}_{h,i} \cdot \mathbf{n}_i|_{\Gamma_{i,j}}$ are the finite element counterparts of vectors $\tilde{\mu}_{i,j}$ and $\tilde{q}_{i,j}$, respectively.

For each interface $\Gamma_{i,j}$, we define an L^2 -orthogonal projection operator $\mathcal{R}_{h,i,j} : L^2(\Gamma_{i,j}) \rightarrow \mathbf{V}_{h,i} \cdot \mathbf{n}_i|_{\Gamma_{i,j}}$ such that, for any $\phi \in L^2(\Gamma_{i,j})$,

$$\langle \phi - \mathcal{R}_{h,i,j}\phi, \mathbf{v} \cdot \mathbf{n}_i \rangle_{\Gamma_{i,j}} = 0 \quad \forall \mathbf{v} \in \mathbf{V}_{h,i}.$$

The operator $\mathcal{R}_{h,j,i} : L^2(\Gamma_{i,j}) \rightarrow \mathbf{V}_{h,j} \cdot \mathbf{n}_j|_{\Gamma_{i,j}}$ is defined analogously. Let $\mathcal{R}_{h,i} : L^2(\partial\Omega_i) \rightarrow \mathbf{V}_{h,i} \cdot \mathbf{n}_i|_{\partial\Omega_i}$ be such that, for any $\phi \in L^2(\partial\Omega_i)$,

$$(\mathcal{R}_{h,i}\phi)|_{\Gamma_{i,j}} = \mathcal{R}_{h,i,j}(\phi|_{\Gamma_{i,j}}).$$

Note that the projection operator $\mathcal{R}_{h,i,j}$ restricted to $\Lambda_{h,i,j}$ acts from the space of piecewise linear functions on $\tilde{\mathcal{E}}_{h,i,j}$ to the space of piecewise constant functions on $\mathcal{E}_{h,i,j}$. Using (4.1), it is clear that the projector $R_{i,j}$ defined on the vector space $\Lambda_{i,j}^d$ is the matrix representation of $\mathcal{R}_{h,i,j} : \Lambda_{h,i,j} \rightarrow \mathbf{V}_{h,i} \cdot \mathbf{n}_i|_{\Gamma_{i,j}}$.

The next step is to reformulate the MFD method in a way that is more suitable for our analysis. Multiplying the first equation in (2.9) by $\vec{v}_i \in X_i^d$, the second one by $\vec{q}_i \in Q_i^{d,0}$, and using the discrete Green's formula (2.8), we get

$$\begin{aligned} [\vec{u}_i, \vec{v}_i]_{X_i^d} - [\vec{p}_i, \mathcal{D}_i^d \vec{v}_i]_{Q_i^d} &= 0 & \forall \vec{v}_i \in X_i^d, \\ [\vec{q}_i, \mathcal{D}IV_i^d \vec{u}_i]_{Q_i^{d,0}} &= [\vec{b}_i, \vec{q}_i]_{Q_i^{d,0}} & \forall \vec{q}_i \in Q_i^{d,0}. \end{aligned} \quad (4.2)$$

Recall that the above equations are coupled with the discrete interface continuity conditions (2.11), (2.12) and the boundary conditions (2.13). Using the isomorphism between the finite element space $\mathbf{V}_{h,i} \times W_{h,i}$ and the vector space $X_i^d \times Q_i^{d,0}$, we define finite element functions $q_{h,i}$, $b_{h,i}$ and $\mathbf{u}_{h,i}$ corresponding to vectors \vec{q}_i , \vec{b}_i and \vec{u}_i , respectively. Then,

$$[\vec{q}_i, \mathcal{D}IV_i^d \vec{u}_i]_{Q_i^{d,0}} = (q_{h,i}, \nabla \cdot \mathbf{u}_{h,i})_{\Omega_i}.$$

The definition of \vec{b}_i implies that

$$[\vec{b}_i, \vec{q}_i]_{Q_i^{d,0}} = (b_{h,i}, q_{h,i})_{\Omega_i} = (b, q_{h,i})_{\Omega_i}.$$

We decompose vector \vec{p}_i as $\vec{p}_i = (\vec{p}_i^0, \vec{p}_i^1)$, where $\vec{p}_i^0 \in Q_i^{d,0}$, and denote the finite element counterparts of \vec{p}_i^0 and $\vec{v}_i \in X_i^d$ by $\vec{p}_{h,i}$ and $\mathbf{v}_{h,i}$, respectively. Let $\lambda_h \in \Lambda_h$ be the mortar finite element counterpart of $\vec{\lambda}$ from the discrete pressure interface continuity condition (2.12). The Dirichlet boundary conditions specify the components of vector \vec{p}_i^1 on $\partial\Omega$. Using (2.7), (2.12), (2.13), and the definition of the projectors $R_{i,j}$ and $\mathcal{R}_{h,i,j}$, we get

$$\begin{aligned} [\vec{p}_i, \mathcal{D}_i^d \vec{v}_i]_{Q_i^d} &= (p_{h,i}, \nabla \cdot \mathbf{v}_{h,i})_{\Omega_i} \\ &\quad - \langle \mathcal{R}_{h,i} \lambda_h, \mathbf{v}_{h,i} \cdot \mathbf{n}_i \rangle_{\Gamma_i} - \langle \mathcal{R}_{h,i} g, \mathbf{v}_{h,i} \cdot \mathbf{n}_i \rangle_{\partial\Omega_i \setminus \Gamma} \\ &= (p_{h,i}, \nabla \cdot \mathbf{v}_{h,i})_{\Omega_i} - \langle \lambda_h, \mathbf{v}_{h,i} \cdot \mathbf{n}_i \rangle_{\Gamma_i} - \langle g, \mathbf{v}_{h,i} \cdot \mathbf{n}_i \rangle_{\partial\Omega_i \setminus \Gamma}. \end{aligned} \quad (4.3)$$

Next, letting $\mu_{h,i,j} \in \Lambda_{h,i,j}$ be the finite element counterpart of vector $\vec{\mu}_{i,j}$, the discrete interface continuity condition (2.10) becomes

$$\langle \mu_{h,i,j}, \mathbf{u}_{h,i} \cdot \mathbf{n}_i \rangle_{\Gamma_{i,j}} = -\langle \mu_{h,i,j}, \mathbf{u}_{h,j} \cdot \mathbf{n}_j \rangle_{\Gamma_{j,i}}.$$

Finally, by introducing the quadrature rule

$$(K^{-1} \mathbf{u}_{h,i}, \mathbf{v}_{h,i})_{h,\Omega_i} \equiv [\vec{u}_i, \vec{v}_i]_{X_i^d},$$

we can reformulate the mortar MFD problem (2.9), (2.12), (2.11) and (2.13) as the following problem. We seek $\mathbf{u}_h \in \mathbf{V}_h$, $p_h \in W_h$, $\lambda_h \in \Lambda_h$ such that, for $1 \leq i \leq n$,

$$\begin{aligned} (K^{-1} \mathbf{u}_h, \mathbf{v})_{h,\Omega_i} &= (p_h, \nabla \cdot \mathbf{v})_{\Omega_i} - \langle \lambda_h, \mathbf{v} \cdot \mathbf{n}_i \rangle_{\Gamma_i} \\ &\quad - \langle g, \mathbf{v} \cdot \mathbf{n}_i \rangle_{\partial\Omega_i \setminus \Gamma} \quad \forall \mathbf{v} \in \mathbf{V}_{h,i}, \end{aligned} \quad (4.4)$$

$$(\nabla \cdot \mathbf{u}_h, w)_{\Omega_i} = (b, w)_{\Omega_i} \quad \forall w \in W_{h,i}, \quad (4.5)$$

$$\sum_{i=1}^n \langle \mathbf{u}_h \cdot \mathbf{n}_i, \mu \rangle_{\Gamma_i} = 0, \quad \forall \mu \in \Lambda_h. \quad (4.6)$$

The next lemma shows that the problem is well posed.

Lemma 4.1 *Assume that for any $\phi \in \Lambda_h$,*

$$\mathcal{R}_{h,i} \phi = 0, \quad 1 \leq i \leq n, \quad \text{implies that} \quad \phi = 0. \quad (4.7)$$

Then there exists a unique solution of (4.4)–(4.6).

Proof The proof closely follows the proof of Lemma 2.1 in [1] with only a slight modification. Since (4.4)–(4.6) is a square system, it is sufficient to show uniqueness. Let $b = 0$ and $g = 0$. Setting $\mathbf{v} = \mathbf{u}_h$, $w = p_h$, and $\mu = -\lambda_h$, adding (4.4)–(4.6), and summing over $1 \leq i \leq n$, implies that

$$\sum_{i=1}^n (K^{-1} \mathbf{u}_h, \mathbf{u}_h)_{h,\Omega_i} = 0.$$

The coercivity result from [5]

$$\sum_{i=1}^n (K^{-1} \mathbf{u}_h, \mathbf{u}_h)_{h, \Omega_i} \geq C \|\mathbf{u}_h\|_{0, \Omega}^2 \quad (4.8)$$

implies that $\mathbf{u}_h = 0$. The argument for proving that $p_h = \lambda_h = 0$ is the same as in the proof of Lemma 2.1 in [1]. \square

Remark 4.1 Above, as well as in several other places in this paper, we employ results obtained in [1]. Although [1] only treats affine elements, it is easy to check that the arguments used to obtain the results referred to here also apply in the case of general quadrilateral elements.

We end this section by noting that (4.8) implies that $(\cdot, \cdot)_h$ is a scalar product that gives rise to a norm $\|\cdot\|_h$ in \mathbf{V}_h . This norm is equivalent to the L^2 -norm, i.e., there exist positive constants c_1 and c_2 independent of h , such that

$$c_1 \|\mathbf{v}\|_{0, \Omega} \leq \|\mathbf{v}\|_h \leq c_2 \|\mathbf{v}\|_{0, \Omega} \quad \forall \mathbf{v} \in \mathbf{V}_h. \quad (4.9)$$

The left inequality is given in (4.8). The right inequality follows from a standard mapping argument, using the equivalence of norms on the reference element \hat{E} .

5 Velocity error estimates for the mortar MFD method

We first recall several projection operators that will be used in the analysis. On each Ω_i there exists a projection Π_i from $(H^1(\Omega_i))^{dim}$ onto $\mathbf{V}_{h,i}$ satisfying

$$(\nabla \cdot (\Pi_i \mathbf{q} - \mathbf{q}), w)_{\Omega_i} = 0 \quad w \in W_{h,i}. \quad (5.1)$$

Let $\Pi : \bigoplus_{i=1}^n (H^1(\Omega_i))^{dim} \rightarrow \mathbf{V}_h$ be defined by $(\Pi \mathbf{q})|_{\Omega_i} = \Pi_i(\mathbf{q}|_{\Omega_i})$. The operator Π is defined locally on each element E by

$$\widehat{\Pi} \mathbf{q} = \hat{\Pi} \hat{\mathbf{q}},$$

where $\hat{\Pi} : (H^1(\hat{E}))^{dim} \rightarrow \hat{\mathbf{V}}(\hat{E})$ is the reference element projection operator satisfying

$$\int_{\hat{f}} (\hat{\Pi} \hat{\mathbf{q}} - \hat{\mathbf{q}}) \cdot \hat{\mathbf{n}} = 0 \quad \forall \hat{f} \subset \partial \hat{E}.$$

Let \mathcal{P}_h be the $L^2(\Gamma)$ projection onto Λ_h satisfying for any $\psi \in L^2(\Gamma)$,

$$\langle \psi - \mathcal{P}_h \psi, \mu \rangle_{\Gamma} = 0 \quad \forall \mu \in \Lambda_h.$$

For any $\varphi \in L^2(\Omega)$, let $\mathcal{Q}_h \varphi \in W_h$ be its $L^2(\Omega)$ projection satisfying

$$(\varphi - \mathcal{Q}_h \varphi, w)_{\Omega} = 0 \quad \forall w \in W_h.$$

We state several well-known approximation properties of these projection operators:

$$\|\psi - \mathcal{P}_h \psi\|_{0, \Gamma_{i,j}} \leq C \|\psi\|_{r, \Gamma_{i,j}} h^r, \quad 0 \leq r \leq 2, \quad (5.2)$$

$$\|\varphi - \mathcal{Q}_h \varphi\|_{0, \Omega_i} \leq C \|\varphi\|_{r, \Omega_i} h^r, \quad 0 \leq r \leq 1, \quad (5.3)$$

$$\|\mathbf{q} - \Pi_i \mathbf{q}\|_{0, \Omega_i} \leq C \|\mathbf{q}\|_{1, \Omega_i} h, \quad (5.4)$$

$$\|\nabla \cdot (\mathbf{q} - \Pi_i \mathbf{q})\|_{0, \Omega_i} \leq C \|\mathbf{q}\|_{r+1, \Omega_i} h^r, \quad 0 \leq r \leq 1, \quad (5.5)$$

where $\|\cdot\|_r$ is the H^r -norm. Bounds (5.2) and (5.3) are standard L^2 -projection approximation results [10]; bounds (5.4) and (5.5) can be found in [7, 25] for affine elements and [27, 28] for quadrilaterals.

We will also make use of the following continuity bound for Π .

Lemma 5.1 *For all elements E and for all $\mathbf{q} \in (H^1(E))^{\dim}$, there exists a constant C independent of h such that*

$$\|\Pi \mathbf{q}\|_{1, E} \leq C \|\mathbf{q}\|_{1, E}.$$

Proof Let us first consider the case of simplicial grids in two and three dimensions. It is well known [24] that for all $E \in \mathcal{T}_h$

$$\|\Pi \mathbf{q}\|_{H(\text{div}; E)} \leq C \|\mathbf{q}\|_{1, E}.$$

The definition of \mathbf{V}_h on simplexes gives that on each E , we have $\nabla \cdot \Pi \mathbf{q} = \frac{1}{\dim} \frac{\partial(\Pi \mathbf{q})_i}{\partial x_i}$, $i = 1, \dots, \dim$, which, combined with the above inequality, implies the assertion of the lemma.

In the case of quadrilateral grids, it follows from the definition of the bilinear mapping that for all $\hat{\mathbf{x}} \in \hat{E}$ and $s = 0, 1$

$$|DF_E(\hat{\mathbf{x}})|_{s, \infty, \hat{E}} \leq Ch, \quad |J_E(\hat{\mathbf{x}})|_{s, \infty, \hat{E}} \leq Ch^2, \quad \left| \frac{1}{J_E} DF_E \right|_{s, \infty, \hat{E}} \leq Ch^{-1}, \quad (5.6)$$

$$|F_E^{-1}|_{1, \infty, \hat{E}} \leq Ch^{-1}, \quad \|J_{F_E^{-1}}\|_{\infty, \hat{E}} \leq Ch^{-2}. \quad (5.7)$$

The rest of the proof is based on the inverse inequality which is not a trivial result for a general quadrilateral. For the sake of completeness, we prove it below. The definition (3.8) implies

$$\int_E \left| \frac{\partial \mathbf{q}}{\partial x_i} \right|^2 d\mathbf{x} = \int_{\hat{E}} \left| \frac{\partial}{\partial x_i} \left(\frac{1}{J_E} DF_E \hat{\mathbf{q}} \right) \right|^2 |J_E| d\hat{\mathbf{x}}.$$

Thus, using (5.6) and (5.7), we get

$$\begin{aligned} \|\mathbf{q}\|_{1, E} &\leq C \left(\left\| \frac{1}{J_E} DF_E \right\|_{\infty, \hat{E}} \|F_E^{-1}\|_{1, \infty, \hat{E}} \|J_E\|_{\infty, \hat{E}}^{1/2} \|\hat{\mathbf{q}}\|_{1, \hat{E}} \right. \\ &\quad \left. + \|J_E\|_{\infty, \hat{E}}^{1/2} \left| \frac{1}{J_E} DF_E \right|_{1, \infty, \hat{E}} \|F_E^{-1}\|_{1, \infty, \hat{E}} \|\hat{\mathbf{q}}\|_{0, \hat{E}} \right) \\ &\leq Ch^{-1} \|\hat{\mathbf{q}}\|_{1, \hat{E}}. \end{aligned} \quad (5.8)$$

Similarly, we get the estimates

$$\|\mathbf{q}\|_{0,E} \leq C \|\hat{\mathbf{q}}\|_{0,\hat{E}} \quad \text{and} \quad \|\hat{\mathbf{q}}\|_{0,\hat{E}} \leq C \|\mathbf{q}\|_{0,E}. \quad (5.9)$$

Combining (5.8) and (5.9) and using the standard inverse inequality on the reference element \hat{E} , we get

$$\|\mathbf{q}\|_{1,E} \leq Ch^{-1} \|\hat{\mathbf{q}}\|_{1,\hat{E}} \leq Ch^{-1} \|\hat{\mathbf{q}}\|_{0,\hat{E}} \leq Ch^{-1} \|\mathbf{q}\|_{0,E},$$

which establishes the inverse inequality for quadrilaterals. Using this inverse inequality, we have

$$\begin{aligned} |\Pi\mathbf{q}|_{1,E} &= |\Pi\mathbf{q} - \mathbf{q}_0|_{1,E} \leq Ch^{-1} \|\Pi\mathbf{q} - \mathbf{q}_0\|_{0,E} \\ &\leq Ch^{-1} (\|\Pi\mathbf{q} - \mathbf{q}\|_{0,E} + \|\mathbf{q} - \mathbf{q}_0\|_{0,E}) \end{aligned}$$

where \mathbf{q}_0 is a constant vector. Let \mathbf{q}_0 be the $L^2(E)$ projection of \mathbf{q} onto the space of constant vectors. Combining the above inequality with the approximation properties (5.3) and (5.4) results in the estimate

$$|\Pi\mathbf{q}|_{1,E} \leq C \|\mathbf{q}\|_{1,E}.$$

The bound $\|\Pi\mathbf{q}\|_{0,E} \leq C \|\mathbf{q}\|_{1,E}$ follows from the approximation property (5.4). This proves the assertion of the lemma. \square

Throughout the paper we will be using the nonstandard trace theorem [14, Theorem 1.5.2.1]

$$\|q\|_{r,\Gamma_{i,j}} \leq C \|q\|_{r+1/2,\Omega_i}.$$

We will also make use of the trace inequality

$$\|\mathbf{v} \cdot \mathbf{n}_i\|_{0,\partial\Omega_i} \leq Ch^{-1/2} \|\mathbf{v}\|_{0,\Omega_i}, \quad \forall \mathbf{v} \in \mathbf{V}_{h,i}, \quad (5.10)$$

which follows from a simple scaling argument.

Let

$$\mathbf{V}_{h,0} = \left\{ \mathbf{v} \in \mathbf{V}_h : \sum_{i=1}^n \langle \mathbf{v}|_{\Omega_i} \cdot \mathbf{n}_i, \mu \rangle_{\Gamma_i} = 0 \quad \forall \mu \in \Lambda_h \right\}$$

be the space of weakly continuous velocities, with respect to the mortar space. Then the mortar MFD method (4.4)–(4.6) can be rewritten in the following way. Find $\mathbf{u}_h \in \mathbf{V}_{h,0}$ and $p_h \in W_h$ such that

$$(K^{-1}\mathbf{u}_h, \mathbf{v})_h = \sum_{i=1}^n (p_h, \nabla \cdot \mathbf{v})_{\Omega_i} - \langle g, \mathbf{v} \cdot \mathbf{n} \rangle_{\partial\Omega}, \quad \forall \mathbf{v} \in \mathbf{V}_{h,0}, \quad (5.11)$$

$$\sum_{i=1}^n (\nabla \cdot \mathbf{u}_h, w)_{\Omega_i} = (b, w), \quad \forall w \in W_h. \quad (5.12)$$

It was shown in [1] that there exists a projection operator Π_0 onto $\mathbf{V}_{h,0}$ such that, for any $\mathbf{q} \in (H^1(\Omega))^{dim}$,

$$(\nabla \cdot (\Pi_0 \mathbf{q} - \mathbf{q}), w)_\Omega = 0 \quad w \in W_h.$$

Moreover, if there exists a constant C , independent of h , such that

$$\begin{aligned} \|\mu\|_{0,\Gamma_{i,j}} &\leq C(\|\mathcal{R}_{h,i}\mu\|_{0,\Gamma_{i,j}} + \|\mathcal{R}_{h,j}\mu\|_{0,\Gamma_{i,j}}) \quad \forall \mu \in \Lambda_h, \\ 1 \leq i &< j \leq n, \end{aligned} \quad (5.13)$$

then Π_0 satisfies the approximation properties

$$\|\Pi_0 \mathbf{q} - \mathbf{q}\|_0 \leq C \sum_{i=1}^n \|\mathbf{q}\|_{r+1/2,\Omega_i} h^{r+1/2}, \quad 0 \leq r \leq 1, \quad (5.14)$$

and

$$\|\Pi_0 \mathbf{q} - \mathbf{q}\|_0 \leq C \sum_{i=1}^n \|\mathbf{q}\|_{1,\Omega_i} h. \quad (5.15)$$

5.1 Optimal convergence estimates for the velocity

We now proceed by proving optimal error estimates for the velocity variable in the mortar MFD method. The analysis is the same for both scalar products (2.3) and (2.4).

Subtracting (5.11)–(5.12) from (3.3)–(3.4) gives the error equations

$$\begin{aligned} (K^{-1}(\Pi \mathbf{u} - \mathbf{u}_h), \mathbf{v})_h &= \sum_{i=1}^n \{ (p - p_h, \nabla \cdot \mathbf{v})_{\Omega_i} - \langle p, \mathbf{v} \cdot \mathbf{n}_i \rangle_{\Gamma_i} \} \\ &\quad + (K^{-1}(\Pi \mathbf{u} - \mathbf{u}), \mathbf{v}) - \sigma(K^{-1} \Pi \mathbf{u}, \mathbf{v}), \end{aligned} \quad (5.16)$$

$$\sum_{i=1}^n (\nabla \cdot (\mathbf{u} - \mathbf{u}_h), w)_{\Omega_i} = 0, \quad (5.17)$$

for any $\mathbf{v} \in \mathbf{V}_{h,0}$ and $w \in W_h$, where

$$\sigma(\mathbf{q}, \mathbf{v}) = (\mathbf{q}, \mathbf{v}) - (\mathbf{q}, \mathbf{v})_h.$$

It was shown in [5] that, $\sigma(\mathbf{q}, \mathbf{v}) = 0$ in the scalar product (2.4) for any $\mathbf{v} \in V_h$ and any constant vector \mathbf{q} . A similar result has been shown in [6] for the scalar product (2.3). Thus, letting \mathbf{q}_0 be the mean value of \mathbf{q} on E , we get

$$|\sigma(\mathbf{q}, \mathbf{v})_E| = |\sigma(\mathbf{q} - \mathbf{q}_0, \mathbf{v})_E| \leq Ch |\mathbf{q}|_{1,E} \|\mathbf{v}\|_{0,E}, \quad E \in \mathcal{T}_h.$$

Therefore,

$$\begin{aligned} |\sigma(K^{-1} \Pi \mathbf{u}, \mathbf{v})| &\leq C \sum_{E \in \mathcal{T}_h} h \|K^{-1}\|_{1,\infty,E} \|\Pi \mathbf{u}\|_{1,E} \|\mathbf{v}\|_{0,E} \\ &\leq C \sum_{i=1}^n h \|K^{-1}\|_{1,\infty,\Omega_i} \|\mathbf{u}\|_{1,\Omega_i} \|\mathbf{v}\|_{0,\Omega_i}, \end{aligned} \quad (5.18)$$

using Lemma 5.1 for the last inequality. Clearly (5.17) implies that

$$\nabla \cdot (\Pi_0 \mathbf{u} - \mathbf{u}_h) = \nabla \cdot (\Pi \mathbf{u} - \mathbf{u}_h) = 0. \quad (5.19)$$

Taking $\mathbf{v} = \Pi_0 \mathbf{u} - \mathbf{u}_h$ in (5.16) we get

$$\begin{aligned} & (K^{-1}(\Pi_0 \mathbf{u} - \mathbf{u}_h), \Pi_0 \mathbf{u} - \mathbf{u}_h)_h \\ &= \sum_{i=1}^n \langle \mathcal{P}_h p - p, (\Pi_0 \mathbf{u} - \mathbf{u}_h) \cdot \mathbf{n}_i \rangle_{\Gamma_i} + (K^{-1}(\Pi \mathbf{u} - \mathbf{u}), \Pi_0 \mathbf{u} - \mathbf{u}_h) \\ & \quad + (K^{-1}(\Pi_0 \mathbf{u} - \Pi \mathbf{u}), \Pi_0 \mathbf{u} - \mathbf{u}_h)_h - \sigma(K^{-1} \Pi \mathbf{u}, \Pi_0 \mathbf{u} - \mathbf{u}_h) \\ & \leq \sum_{i=1}^n \|\mathcal{P}_h p - p\|_{0, \Gamma_i} \|(\Pi_0 \mathbf{u} - \mathbf{u}_h) \cdot \mathbf{n}_i\|_{0, \Gamma_i} \\ & \quad + (K^{-1}(\Pi \mathbf{u} - \mathbf{u}), \Pi_0 \mathbf{u} - \mathbf{u}_h) + (K^{-1}(\Pi_0 \mathbf{u} - \Pi \mathbf{u}), \Pi_0 \mathbf{u} - \mathbf{u}_h)_h \\ & \quad + |\sigma(K^{-1} \Pi \mathbf{u}, \Pi_0 \mathbf{u} - \mathbf{u}_h)| \\ & \leq C \left(\sum_{i=1}^n \|p\|_{2, \Omega_i} h^{3/2} \|\Pi_0 \mathbf{u} - \mathbf{u}_h\|_{0, \Omega_i} h^{-1/2} \right. \\ & \quad \left. + \sum_{i=1}^n \|K^{-1}\|_{1, \infty, \Omega_i} \|\mathbf{u}\|_{1, \Omega_i} h \|\Pi_0 \mathbf{u} - \mathbf{u}_h\|_0 \right), \quad (5.20) \end{aligned}$$

where we used (5.2), (5.10), (5.4), (5.14), and (5.18) for the last inequality. With (5.19)–(5.20), (4.9), (5.5), and (5.15) we have shown the following theorem.

Theorem 5.1 *Let $K^{-1} \in W^{1, \infty}(\Omega_i)$, $1 \leq i \leq n$, and let (4.7) hold. Then, for the velocity \mathbf{u}_h of the mortar mimetic finite difference method (4.4)–(4.6), there exists a positive constant C independent of h such that*

$$\|\nabla \cdot (\mathbf{u} - \mathbf{u}_h)\|_0 \leq C \sum_{i=1}^n \|\mathbf{u}\|_{2, \Omega_i} h.$$

Moreover, if (5.13) holds, then

$$\|\mathbf{u} - \mathbf{u}_h\|_0 \leq C \sum_{i=1}^n (\|p\|_{2, \Omega_i} + \|\mathbf{u}\|_{1, \Omega_i}) h.$$

5.2 Superconvergence for the velocity

In this section, we show that in the case of h^2 -uniform quadrilateral grids the velocity converges with an order one-half higher than the $O(h)$ in a discrete L^2 -norm. This superconvergence result for non-matching grids rests on conforming grids superconvergence results in [6] and [12] for MFD and MFE methods, respectively, and our analysis in Section 5.1. Although this superconvergence result is weaker than the $O(h^2)$ superconvergence result in [6], it is consistent with the superconvergence result for mortar MFE methods [31, 1]. We also note that this result is proved only for the scalar product (2.3).

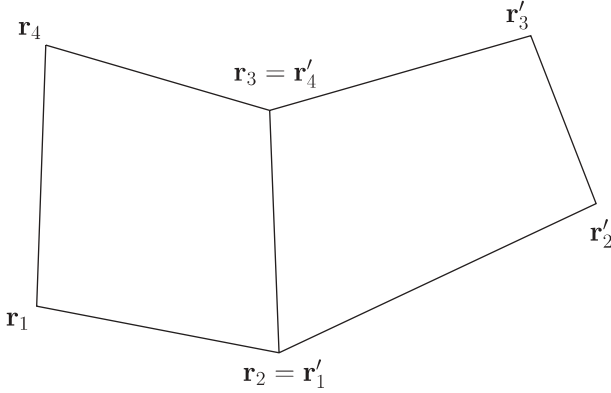


Fig. 4 h^2 -uniform quadrilateral grid

Referring to Fig. 4, a quadrilateral partition is called h^2 -uniform if each element is an h^2 -parallelogram, i.e., $\|(\mathbf{r}_2 - \mathbf{r}_1) - (\mathbf{r}_3 - \mathbf{r}_4)\| \leq Ch^2$, and any two adjacent quadrilaterals form an h^2 -parallelogram, i.e., $\|(\mathbf{r}_2 - \mathbf{r}_1) - (\mathbf{r}'_2 - \mathbf{r}'_1)\| \leq Ch^2$.

To establish superconvergence, we modify the last inequality in (5.20). In particular, (5.2) gives

$$\begin{aligned} & \sum_{i=1}^n \|\mathcal{P}_h p - p\|_{0,\Gamma_i} \|(\Pi_0 \mathbf{u} - \mathbf{u}_h) \cdot \mathbf{n}_i\|_{0,\Gamma_i} \\ & \leq C \sum_{i=1}^n \|p\|_{5/2,\Omega_i} h^2 \|\Pi_0 \mathbf{u} - \mathbf{u}_h\|_{0,\Omega_i} h^{-1/2}, \end{aligned}$$

and (5.14) gives

$$(K^{-1}(\Pi_0 \mathbf{u} - \Pi \mathbf{u}), \Pi_0 \mathbf{u} - \mathbf{u}_h)_h \leq C \sum_{i=1}^n \|\mathbf{u}\|_{3/2,\Omega_i} h^{3/2} \|\Pi_0 \mathbf{u} - \mathbf{u}_h\|_0.$$

In addition, [12, Theorem 5.1] implies

$$(K^{-1}(\Pi \mathbf{u} - \mathbf{u}), \Pi_0 \mathbf{u} - \mathbf{u}_h) \leq C \sum_{i=1}^n \|K^{-1}\|_{2,\infty,\Omega_i} \|\mathbf{u}\|_{2,\Omega_i} h^2 \|\Pi_0 \mathbf{u} - \mathbf{u}_h\|_0,$$

and [6, Lemma 4.3] gives

$$|\sigma(K^{-1} \Pi \mathbf{u}, \Pi_0 \mathbf{u} - \mathbf{u}_h)| \leq C \sum_{i=1}^n \|K^{-1}\|_{2,\infty,\Omega_i} \|\mathbf{u}\|_{2,\Omega_i} h^2 \|\Pi_0 \mathbf{u} - \mathbf{u}_h\|_0.$$

Combining the above four bounds, we arrive at the following superconvergence result.

Theorem 5.2 *Let $K^{-1} \in W^{2,\infty}(\Omega_i)$, $1 \leq i \leq n$, and let (5.13) hold. Then, for the velocity \mathbf{u}_h of the mortar mimetic finite difference method (4.4)–(4.6) with the scalar product (2.3) on h^2 -uniform quadrilateral grids, there exists a positive constant C independent of h such that*

$$\|\Pi\mathbf{u} - \mathbf{u}_h\|_0 \leq C \sum_{i=1}^n (\|p\|_{5/2,\Omega_i} + \|\mathbf{u}\|_{2,\Omega_i}) h^{3/2}.$$

The above result can be applied to obtain superconvergence for the computed velocity to the average edge fluxes. Define, for any $\mathbf{v} \in (H^1(\Omega_i))^2$, $i = 1, \dots, n$,

$$|||\mathbf{v}|||^2 = \sum_{E \in \mathcal{T}_h} |||\mathbf{v}|||_E^2, \quad |||\mathbf{v}|||_E^2 = \sum_{k=1}^4 \left(\int_{e_k} \mathbf{v} \cdot \mathbf{n}_k \, ds \right)^2. \quad (5.21)$$

It is easy to see [6] that $|||\cdot|||$ is a norm on \mathbf{V}_h and there exist constants c_1 and c_2 independent of h such that

$$c_1 \|\mathbf{v}\|_{0,\Omega} \leq |||\mathbf{v}||| \leq c_2 \|\mathbf{v}\|_{0,\Omega} \quad \forall \mathbf{v} \in \mathbf{V}_h. \quad (5.22)$$

Moreover, $|||\Pi\mathbf{v} - \mathbf{v}||| = 0$ for any $\mathbf{v} \in (H^1(\Omega_i))^2$, $i = 1, \dots, n$. We have the following superconvergence result.

Theorem 5.3 *Under the assumptions of Theorem 5.2, there exists a positive constant C independent of h such that*

$$|||\mathbf{u} - \mathbf{u}_h||| \leq C \sum_{i=1}^n (\|p\|_{5/2,\Omega_i} + \|\mathbf{u}\|_{2,\Omega_i}) h^{3/2}.$$

Proof By the triangle inequality and (5.22),

$$|||\mathbf{u} - \mathbf{u}_h||| \leq |||\Pi\mathbf{u} - \mathbf{u}_h||| \leq c_2 \|\Pi\mathbf{u} - \mathbf{u}_h\|_0,$$

and the assertion of the theorem follows from Theorem 5.2. \square

6 Pressure error estimates for the mortar MFD method

In this section, we employ a duality argument to obtain superconvergence for $\mathcal{Q}_h p - p_h$ and optimal convergence for $p - p_h$ in the mortar MFD method. To the best of our knowledge, these are the first pressure superconvergence results for the MFD methods.

The estimates are proved for both scalar products (2.3) and (2.4) on triangular, tetrahedral and h^2 -uniform quadrilateral meshes. In the case of general quadrilateral meshes, the superconvergence estimate is shown only for the the scalar product (2.4).

We first derive a superconvergence estimate for the quadrature error, which will be used in the proof of the main result.

Lemma 6.1 *Let $K^{-1} \in W^{2,\infty}(\Omega_i)$, $1 \leq i \leq n$. Then, for all $\mathbf{v}, \mathbf{q} \in \mathbf{V}_h$, there exists a positive constant C independent of h such that*

$$|\sigma(K^{-1}\mathbf{v}, \mathbf{q})| \leq C \sum_{E \in \mathcal{T}_h} h^r \|\mathbf{v}\|_{1,E} \|\mathbf{q}\|_{1,E}$$

where, for the scalar product (2.3), $r = 2$ on simplicial grids and h^2 -uniform quadrilateral grids, and $r = 1$ on general quadrilateral grids. If the scalar product is given by (2.4), then $r = 2$ on simplicial grids and general quadrilateral grids.

Proof For an element $E \in \mathcal{T}_h$, we define the error

$$\sigma_E(K^{-1}\mathbf{v}, \mathbf{q}) = \int_E K^{-1}\mathbf{v} \cdot \mathbf{q} \, dx - (K^{-1}\mathbf{v}, \mathbf{q})_{h,E}. \quad (6.1)$$

First, we consider the scalar product $(K^{-1}\mathbf{v}, \mathbf{q})_{h,E}$ given by (2.3). It was shown in [5] that $\sigma_E(\mathbf{v}_0, \mathbf{q}) = 0$ for all constant vectors \mathbf{v}_0 . Using this result and the symmetry of (6.1), we get

$$\begin{aligned} \sigma_E(K^{-1}\mathbf{v}, \mathbf{q}) &= \sigma_E(K^{-1}\mathbf{v}, \mathbf{q} - \mathbf{q}_0) + \sigma_E((K^{-1} - K_0^{-1})(\mathbf{v} - \mathbf{v}_0), \mathbf{q}_0) \\ &\quad + \sigma_E(K^{-1}\mathbf{v}_0, \mathbf{q}_0) \end{aligned} \quad (6.2)$$

where $\mathbf{v}_0, \mathbf{q}_0$ are constant vectors and K_0 is a constant tensor. By a constant vector (tensor) we mean a vector (tensor) with constant components. Let \mathbf{v}_0 and \mathbf{q}_0 be the $L^2(E)$ orthogonal projections of \mathbf{v} and \mathbf{q} , respectively, onto the space of constant vectors, let $K_0^{-1} \equiv K_E^{-1} = K^{-1}(m_E)$, where m_E is the center of gravity of E , and let $(K^{-1}\mathbf{v})_0$ be the $L^2(E)$ projection of $K^{-1}\mathbf{v}$ into the space of constant vectors. Using the Taylor's theorem, it is easy to verify that

$$\|K^{-1} - K_0^{-1}\|_{\infty,E} \leq Ch \|K^{-1}\|_{1,\infty,E}$$

Using (2.5) and (5.3), we get for the first term on the right in (6.2)

$$\begin{aligned} |\sigma_E(K^{-1}\mathbf{v}, \mathbf{q} - \mathbf{q}_0)| &= |\sigma_E(K^{-1}\mathbf{v} - (K^{-1}\mathbf{v})_0, \mathbf{q} - \mathbf{q}_0)| \\ &\leq Ch^2 \|K^{-1}\|_{1,\infty,E} \|\mathbf{v}\|_{1,E} \|\mathbf{q}\|_{1,E}. \end{aligned}$$

The second term in (6.2) is estimated as

$$\begin{aligned} |\sigma_E((K^{-1} - K_0^{-1})(\mathbf{v} - \mathbf{v}_0), \mathbf{q}_0)| &\leq C \|K^{-1} - K_0^{-1}\|_{\infty,E} \|\mathbf{v} - \mathbf{v}_0\|_{0,E} \|\mathbf{q}_0\|_{0,E} \\ &\leq Ch^2 \|K\|_{1,\infty,E} \|\mathbf{v}\|_{1,E} \|\mathbf{q}\|_{0,E}, \end{aligned} \quad (6.3)$$

The remaining term in (6.2) can be rewritten as

$$\begin{aligned} \sigma_E(K^{-1}\mathbf{v}_0, \mathbf{q}_0) &= \int_E K^{-1}\mathbf{v}_0 \cdot \mathbf{q}_0 \, dx - (K^{-1}\mathbf{v}_0, \mathbf{q}_0)_{h,E} \\ &= \overline{K^{-1}\mathbf{v}_0 \cdot \mathbf{q}_0}|E| - \frac{1}{\alpha_E} \sum_{j=1}^s |T_j| K^{-1}(\mathbf{r}_j) \mathbf{v}_0 \cdot \mathbf{q}_0, \end{aligned}$$

where $\overline{K^{-1}}$ is the mean value of K^{-1} on E , $\alpha_E = 2$ for quadrilaterals, $\alpha_E = 3$ for triangles, $\alpha_E = 4$ for tetrahedra, and s is the number of vertices of element E . For simplicial elements, $|T_j| = |E|$ and it is easy to check that the quadrature is exact for linear tensors. An application of the Bramble-Hilbert lemma gives

$$\begin{aligned} |\sigma_E(K^{-1}\mathbf{v}_0, \mathbf{q}_0)| &\leq Ch^2|K^{-1}\mathbf{v}_0|_{2,E}\|\mathbf{q}_0\|_{0,E} \\ &\leq Ch^2|K^{-1}|_{2,\infty,E}\|\mathbf{v}_0\|_{0,E}\|\mathbf{q}_0\|_{0,E}. \end{aligned} \quad (6.4)$$

For general quadrilaterals, the quadrature is exact for constant tensors and we have

$$|\sigma_E(K^{-1}\mathbf{v}_0, \mathbf{q}_0)| = |\sigma_E((K^{-1} - K_0^{-1})\mathbf{v}_0, \mathbf{q}_0)| \leq Ch\|K^{-1}\|_{1,\infty,E}\|\mathbf{v}_0\|_{0,E}\|\mathbf{q}_0\|_{0,E}$$

We now show that this term is $O(h^2)$ in the case of h^2 -parallelograms. To do this we map it to the reference element. It follows from (3.5) that $J_E(\hat{\mathbf{r}}_j) = 2|T_j|$. Thus,

$$\begin{aligned} (K^{-1}\mathbf{v}_0, \mathbf{q}_0)_{h,E} &= \frac{1}{2} \sum_{j=1}^4 |T_j| K^{-1}(\mathbf{r}_j) \mathbf{v}_0 \cdot \mathbf{q}_0 = \frac{1}{2} \sum_{j=1}^4 |T_j| \hat{K}^{-1}(\hat{\mathbf{r}}_j) \mathbf{v}_0 \cdot \mathbf{q}_0 \\ &= \frac{1}{4} \sum_{j=1}^4 B_E(\hat{\mathbf{r}}_j) \mathbf{v}_0 \cdot \mathbf{q}_0 \equiv (B_E \mathbf{v}_0, \mathbf{q}_0)_T, \end{aligned} \quad (6.5)$$

where $B_E = J_E \hat{K}^{-1}$. Note that the quadrature rule $(\cdot, \cdot)_T$ is the trapezoidal rule on the reference square \hat{E} .

For the integral term in the quadrature error we write

$$\int_E K^{-1} \mathbf{v}_0 \cdot \mathbf{q}_0 \, dx = \int_{\hat{E}} \hat{K}^{-1} \mathbf{v}_0 \cdot \mathbf{q}_0 J_E \, d\hat{x} = \int_{\hat{E}} B_E \mathbf{v}_0 \cdot \mathbf{q}_0 \, d\hat{x}. \quad (6.6)$$

Using (6.5) and (6.6) we obtain

$$\sigma_E(K^{-1}\mathbf{v}_0, \mathbf{q}_0) = \int_{\hat{E}} B_E \mathbf{v}_0 \cdot \mathbf{q}_0 \, d\hat{x} - (B_E \mathbf{v}_0, \mathbf{q}_0)_T \equiv \sigma_{\hat{E}}(B_E \mathbf{v}_0, \mathbf{q}_0). \quad (6.7)$$

Since the trapezoidal quadrature rule on \hat{E} is exact for linear polynomials, the Bramble-Hilbert lemma implies that

$$|\sigma_{\hat{E}}(B \mathbf{v}_0, \mathbf{q}_0)| \leq C|B|_{2,\infty,\hat{E}}\|\mathbf{v}_0\|_{0,\hat{E}}\|\mathbf{q}_0\|_{0,\hat{E}} \quad (6.8)$$

To bound on $|B|_{2,\infty,\hat{E}}$, we note that for an h^2 -parallelogram

$$|J_E|_{1,\infty,\hat{E}} \leq Ch^3, \quad |J_E|_{2,\infty,\hat{E}} = 0, \quad |F_E|_{s,\infty,\hat{E}} \leq Ch^s, \quad s = 1, 2.$$

Therefore,

$$|B|_{2,\infty,\hat{E}} \leq C \left(h^3 |\hat{K}^{-1}|_{1,\infty,\hat{E}} + h^2 |\hat{K}^{-1}|_{2,\infty,\hat{E}} \right) \leq Ch^4 \|K^{-1}\|_{2,\infty,E},$$

using the chain rule for the last inequality. The above bound, combined with (6.7) and (6.8), implies

$$\begin{aligned} |\sigma_E(K^{-1}\mathbf{v}_0, \mathbf{q}_0)| &\leq Ch^4 \|K^{-1}\|_{2,\infty,E} \|\mathbf{v}_0\|_{0,\hat{E}} \|\mathbf{q}_0\|_{0,\hat{E}} \\ &\leq Ch^2 \|K^{-1}\|_{2,\infty,E} \|\mathbf{v}\|_{0,E} \|\mathbf{q}\|_{0,E}, \end{aligned}$$

which completes the proof in the case of the scalar product (2.3).

Let the scalar product $(K^{-1}\mathbf{v}, \mathbf{q})_{h,E}$ be given by (2.4). The only difference in this case is the estimate of the third term in (6.2). Note that the scalar product

$$(K^{-1}\mathbf{v}_0, \mathbf{q}_0)_{h,E} = \frac{1}{\alpha_E} \sum_{j=1}^s |T_j| K_E^{-1} \mathbf{v}_0 \cdot \mathbf{q}_0 = |E| K_E^{-1} \mathbf{v}_0 \cdot \mathbf{q}_0$$

is exact for linear tensors for both simplicial and quadrilateral elements. The application of the Bramble-Hilbert lemma gives estimate (6.4). \square

We continue with the duality argument for bounding $\|\mathcal{Q}_h p - p_h\|_0$. We first rewrite the error equation (5.16) as follows:

$$\begin{aligned} &(K^{-1}(\mathbf{u} - \mathbf{u}_h), \mathbf{v}) \\ &= \sum_{i=1}^n ((p - p_h, \nabla \cdot \mathbf{v})_{\Omega_i} - \langle p, \mathbf{v} \cdot \mathbf{n}_i \rangle_{\Gamma_i}) - \sigma(K^{-1}\mathbf{u}_h, \mathbf{v}) \end{aligned} \quad (6.9)$$

Let φ be the solution of

$$\begin{aligned} -\nabla \cdot K \nabla \varphi &= -(\mathcal{Q}_h p - p_h) && \text{in } \Omega, \\ \varphi &= 0 && \text{on } \partial\Omega. \end{aligned}$$

We assume that this problem has H^2 -elliptic regularity. This is true, for example if the components of $K \in C^{0,1}(\overline{\Omega})$ and Ω is convex or $\partial\Omega$ is smooth enough (see [14, 18]). Then, we have

$$\|\varphi\|_2 \leq C \|\mathcal{Q}_h p - p_h\|_0. \quad (6.10)$$

Take $\mathbf{v} = \Pi_0 K \nabla \varphi$ in (6.9) to get

$$\begin{aligned} \|\mathcal{Q}_h p - p_h\|_0^2 &= \sum_{i=1}^n (\mathcal{Q}_h p - p_h, \nabla \cdot \Pi_0 K \nabla \varphi)_{\Omega_i} \\ &= \sum_{i=1}^n \{ (K^{-1}(\mathbf{u} - \mathbf{u}_h), \Pi_0 K \nabla \varphi)_{\Omega_i} + \langle p - \mathcal{P}_h p, \Pi_0 K \nabla \varphi \cdot \mathbf{n}_i \rangle_{\Gamma_i} \} \\ &\quad + \sigma(K^{-1}\mathbf{u}_h, \Pi_0 K \nabla \varphi). \end{aligned} \quad (6.11)$$

The first two terms on the right in (6.11) appear also in the proof of Theorem 5.1 in [1], where it was shown that

$$\begin{aligned} &\sum_{i=1}^n \{ (K^{-1}(\mathbf{u} - \mathbf{u}_h), \Pi_0 K \nabla \varphi)_{\Omega_i} + \langle p - \mathcal{P}_h p, \Pi_0 K \nabla \varphi \cdot \mathbf{n}_i \rangle_{\Gamma_i} \} \\ &\leq C \sum_{i=1}^n h^2 \|K\|_{1,\infty,\Omega_i} (\|p\|_{2,\Omega_i} + \|\mathbf{u}\|_{2,\Omega_i}) \|\varphi\|_{2,\Omega_i}. \end{aligned} \quad (6.12)$$

Using Lemma 6.1, the last term in (6.11) can be bounded as

$$\begin{aligned}
& |\sigma(K^{-1}\mathbf{u}_h, \Pi_0 K \nabla \varphi)| \\
& \leq C \sum_{E \in \mathcal{T}_h} h^r \|\mathbf{u}_h\|_{1,E} \|\Pi_0 K \nabla \varphi\|_{1,E} \\
& \leq C \sum_{E \in \mathcal{T}_h} h^r (\|\mathbf{u}_h - \Pi \mathbf{u}\|_{1,E} + \|\Pi \mathbf{u}\|_{1,E}) \\
& \quad \times (\|\Pi_0 K \nabla \varphi - \Pi K \nabla \varphi\|_{1,E} + \|\Pi K \nabla \varphi\|_{1,E}) \\
& \leq C \sum_{E \in \mathcal{T}_h} h^r (h^{-1} \|\mathbf{u}_h - \Pi \mathbf{u}\|_{0,E} + \|\mathbf{u}\|_{1,E}) \\
& \quad \times (h^{-1} \|\Pi_0 K \nabla \varphi - \Pi K \nabla \varphi\|_{0,E} + \|K \nabla \varphi\|_{1,E}) \\
& \leq C \sum_{i=1}^n h^r \|K\|_{1,\infty,\Omega_i} (\|p\|_{2,\Omega_i} + \|\mathbf{u}\|_{1,\Omega_i}) \|\varphi\|_{2,\Omega_i}, \quad (6.13)
\end{aligned}$$

where we used the inverse inequality and Lemma 5.1 in the third inequality, and Theorem 5.1 and (5.14) in the last inequality. A combination of (6.10)–(6.13) gives the following result.

Theorem 6.1 *Let $K \in W^{1,\infty}(\Omega_i)$, $K^{-1} \in W^{2,\infty}(\Omega_i)$, $1 \leq i \leq n$, and (5.13) hold. Then, for the pressure p_h of the mortar mimetic finite difference method (4.4)–(4.6), there exists a constant C independent of h such that*

$$\begin{aligned}
\|\mathcal{Q}_h p - p_h\|_0 & \leq C \sum_{i=1}^n (\|p\|_{2,\Omega_i} + \|\mathbf{u}\|_{2,\Omega_i}) h^r, \\
\|p - p_h\|_0 & \leq C \sum_{i=1}^n (\|p\|_{2,\Omega_i} + \|\mathbf{u}\|_{2,\Omega_i}) h,
\end{aligned}$$

where, for scalar product (2.3), $r = 2$ on simplicial grids and h^2 -uniform quadrilateral grids, and $r = 1$ on general quadrilateral grids. If the scalar product is given by (2.4), then $r = 2$ on simplicial grids and general quadrilateral grids.

7 Numerical experiments

In this section, we confirm our theoretical estimates for locally refined meshes, which can be viewed as a special case of non-matching meshes. An example of a computational mesh is shown in Fig. 5. This mesh consists of 13 quadrilateral subdomains with different levels of uniform refinement. We study convergence of the mortar MFD method using the sequence of meshes that is generated by uniform refinement (and coarsening) of this mesh.

We generated another sequence of meshes from the above sequence by perturbing the positions of mesh nodes. A mesh node is moved to a random position inside a square centered around its initial position. The sides of the square are aligned with the coordinate axes and are equal in length to 40% of the length of the smallest

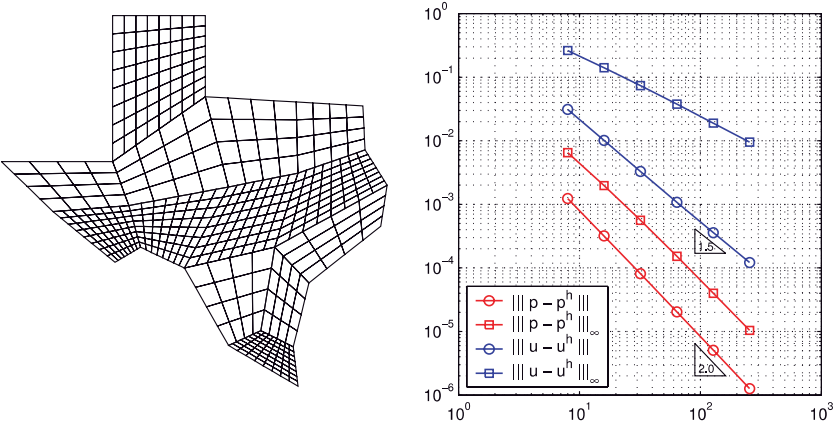


Fig. 5 Convergence rates on smooth meshes

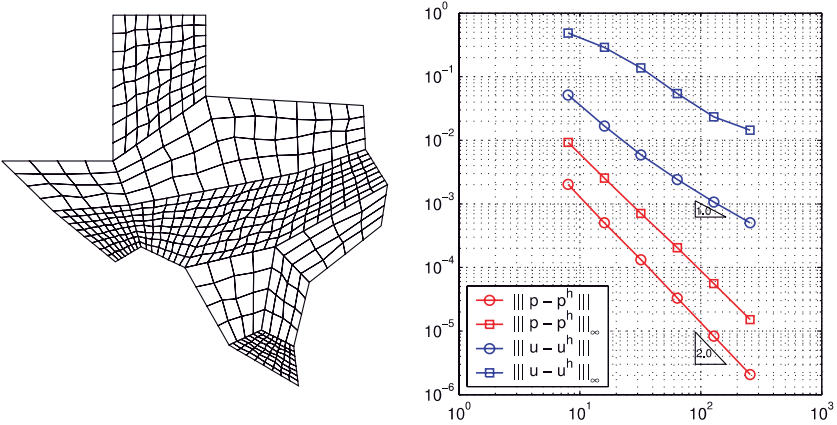


Fig. 6 Convergence rates on random meshes

edge adjacent to the node. The positions of mesh nodes on the domain boundary and on subdomain interfaces are not perturbed. An example of such a random mesh is shown in Fig. 6.

The discrete interface continuity conditions for the mortar MFD method are drastically simplified in the case of locally refined meshes. We consider the interface $\Gamma_{i,j}$ and denote by $\mathcal{E}_{h,i,j}$ the finer of its two adjacent partitions. Assume $\tilde{\mathcal{E}}_{h,i,j} = \mathcal{E}_{h,j,i}$, and set the mortar space $\Lambda_{h,i,j}$ to be the space of discontinuous piecewise linear functions. To describe projectors $R_{i,j}$ and $R_{j,i}$, it is sufficient to consider a three-cell interface. Let cells E_1 and E_2 from $\mathcal{T}_{h,i}$ be adjacent to a cell E_3 from $\mathcal{T}_{h,j}$. Without loss of generality, we assume that $\mathcal{E}_{h,i,j} = \{f_1, f_2\}$ and $\mathcal{E}_{h,j,i} = \{f_3\}$. Then, the dimension of the mortar space is 2, $R_{i,j}$ is a 2×2 matrix, and $R_{j,i}$ is a 1×2 matrix. It is easy to check that definition (4.1) implies

$$R_{i,i} = \frac{1}{2|f_3|} \begin{bmatrix} |f_1| & |f_2| + |f_3| \\ |f_1| + |f_3| & |f_2| \end{bmatrix} \quad \text{and} \quad R_{j,i} = \frac{1}{2} [1 \ 1].$$

Eliminating vector $\vec{\lambda}$ from (2.12), we get discrete interface continuity conditions

$$|f_1|p_{f_1} + |f_2|p_{f_2} = |f_3|p_{f_3} \quad \text{and} \quad u_{f_1} = u_{f_2} = -u_{f_3}.$$

The velocity condition is similar to the condition proposed and analyzed numerically in [19], where it was shown that the resulting MFD method is exact for linear solutions. This condition is also closely related to the “slave” or “worker” nodes local refinement technique in MFE methods [11, 13].

In this example, we set $p(x, y) = x^3y^2 + x \cos(xy) \sin(x)$ to be the exact solution and K to be the full tensor

$$K(x, y) = \begin{pmatrix} (x+1)^2 + y^2 & -xy \\ -xy & (x+1)^2 \end{pmatrix}.$$

The computational domain is located at the positive quadrant ($x > 0, y > 0$) of the XY-plane which implies that tensor K is a positive definite matrix.

The right pictures in Fig. 5 and 6 show convergence rates for pressure and velocity. We demonstrate convergence in discrete L_2 and maximum norms. The discrete L_2 norm for the velocity variable is defined in (5.21) and the maximum norm is given by

$$|||\mathbf{u} - \mathbf{u}_h|||_\infty = \max_{f \in \mathcal{T}_h} \left| \frac{1}{|f|} \int_f \mathbf{u} \cdot \mathbf{n}_f \, ds - \mathbf{u}_h \cdot \mathbf{n}_f \right|.$$

Convergence of the pressure variable is shown in the following discrete norms:

$$|||p - p_h||| = \left(\sum_{E \in \mathcal{T}_h} |p(m_E) - p_h(m_E)|^2 |E| \right)^{1/2}$$

and

$$|||p - p_h|||_\infty = \max_{E \in \mathcal{T}_h} |p(m_E) - p_h(m_E)|.$$

The uniform refinement of a quadrilateral results in a h^2 -uniform mesh. Therefore, the mortar MFD method with scalar product (2.3) is used on the sequence of smooth meshes (see Figure 5). We observe 1.5 convergence rate for the velocity variable which was predicted in Theorem 5.3.

The mortar MFD method with scalar product (2.4) is used on the sequence of random meshes (see Figure 6). The method exhibits the asymptotically optimal first order convergence rate for the velocity. This result is in agreement with the assertion of Theorem 5.1.

The second order convergence rate for the pressure variable in the discrete L_2 norm is observed in both experiments. This confirms the results of Theorem 6.1.

8 Conclusions

In this paper we develop the mortar MFD method on non-matching multiblock grids. We establish a relation between the mortar MFD and mortar MFE methods. We use this relation to prove optimal convergence results for both the pressure and the velocity on quadrilateral, triangular, and tetrahedral grids. In addition, we establish superconvergence for the pressure at cell centers and, in the case of h^2 -uniform quadrilateral grids, superconvergence for the normal velocities at the midpoints of edges. Our approach can be generalized to polygonal non-matching meshes using recent advances in the theory of MFD and MFE methods (see [17, 8]).

References

1. Arbogast, T., Cowsar, L.C., Wheeler, M.F., Yotov, I.: Mixed finite element methods on non-matching multiblock grids. *SIAM J. Numer. Anal.* **37**(4), 1295–1315 (2000)
2. Arbogast, T., Dawson, C.N., Keenan, P.T., Wheeler, M.F., Yotov, I.: Enhanced cell-centered finite differences for elliptic equations on general geometry. *SIAM J. Sci. Comp.* **19**(2), 404–425 (1998)
3. Ben Belgacem, F.: The mortar finite element method with Lagrange multipliers. *Numer. Math.* **84**(2), 173–197 (1999)
4. Bernardi, C., Maday, Y., Patera, A.T.: A new nonconforming approach to domain decomposition: the mortar element method. *Nonlinear partial differential equations and their applications* In: H. Brezis and J. L. Lions (eds.) Longman Scientific & Technical UK 1994
5. Berndt, M., Lipnikov, K., Moulton, J.D., Shashkov, M.: Convergence of mimetic finite difference discretizations of the diffusion equation. *East-West J. Numer. Math.* **9**, 253–284 (2001)
6. Berndt, M., Lipnikov, K., Shashkov, M., Wheeler, M.F., Yotov, I.: Superconvergence of the velocity in mimetic finite difference methods on quadrilaterals. *SIAM J. Numer. Anal.* to appear
7. Brezzi, F., Fortin, M.: *Mixed and hybrid finite element methods*. Springer-Verlag, New York 1991
8. Brezzi, F., Lipnikov, K., Shashkov, M.: Convergence of mimetic finite difference method for diffusion problems on polyhedral meshes. *SIAM J. Numer. Anal.* to appear
9. Campbell, J., Shashkov, M.: A tensor artificial viscosity using a mimetic finite difference algorithm. *J. Comput. Phys.* **172**, 739–765 (2001)
10. Ciarlet, P.G.: *The finite element method for elliptic problems*. North-Holland, New York, 1978
11. Ewing, R.E., Lazarov, R.D., Russell, T.F., Vassilevski, P.S.: Analysis of the mixed finite element method for rectangular Raviart-Thomas elements with local refinement. In: *Third International Symposium on Domain Decomposition Methods for Partial Differential Equations* T.F. Chan and R. Glowinski and J. Periaux and O. B. Widlund (Eds.), SIAM Philadelphia 1990 pp 98–114
12. Ewing, R.E., Liu, M., Wang, J.: Superconvergence of mixed finite element approximations over quadrilaterals. *SIAM J. Numer. Anal.* **36**(3) 772–787 (1999)
13. Ewing, R.E., Wang, J.: Analysis of mixed finite element methods on locally refined grids. *Numer. Math.* **63**, 183–194 (1992)
14. Grisvard, P.: *Elliptic problems in nonsmooth domains*. Pitman, Boston, 1985
15. Hyman, J., Morel, J., Shashkov, M., Steinberg, S.: Mimetic finite difference methods for diffusion equations. *Comp. Geosci.* **6**(3–4), 333–352 (2002)
16. Hyman, J.M., Shashkov, M., Steinberg, S.: The numerical solution of diffusion problems in strongly heterogeneous non-isotropic materials. *J. Comput. Phys.* **132**, 130–148 (1997)
17. Kuznetsov, Y., Repin, S.: Convergence analysis and error estimates for mixed finite element method on distorted meshes. *J. Numer. Math.* **13**(1), 33–51 (2005)
18. J. L. Lions and E. Magenes *Non-homogeneous boundary value problems and applications* Springer-Verlag, **1**, 1972

19. Lipnikov, K., Morel, J., Shashkov, M.: Mimetic finite difference methods for diffusion equations on non-orthogonal non-conformal meshes. *J. Comput. Phys.* **199**, 589–597 (2004)
20. Margolin, L., Shashkov, M., Smolarkiewicz, P.: A discrete operator calculus for finite difference approximations. *Comput. Meth. Appl. Mech. Engrg.* **187**, 365–383 (2000)
21. Morel, J.E., Roberts, R.M., Shashkov, M.: A local support-operators diffusion discretization scheme for quadrilateral $r - z$ meshes. *J. Comput. Phys.* **144**, 17–51 (1998)
22. Nedelec, J.C.: Mixed finite elements in \mathbf{R}^3 . *Numer. Math.* **35**, 315–341 (1980)
23. Peszyńska, M., Wheeler, M.F., Yotov, I.: Mortar upscaling for multiphase flow in porous media. *Comput. Geosci. Comput. Geosci.* **6**(1), 73–100 (2002)
24. Raviart, R.A., Thomas, J.M.: A mixed finite element method for 2nd order elliptic problems. In: *Mathematical Aspects of the Finite Element Method Lecture Notes in Mathematics* Springer-Verlag, New York **606**, 1977 pp 292–315
25. Roberts, J.E., Thomas, J.-M.: Mixed and hybrid methods. In *Handbook of Numerical Analysis* Vol. **II** Elsevier Science Publishers B.V. 1991 P. G. Ciarlet and J.L. Lions pp 523–639
26. Shashkov, M., Steinberg, S.: Solving diffusion equations with rough coefficients in rough grids. *J. Comput. Phys.* **129**, 383–405 (1996)
27. Thomas, J.M.: *Sur l'analyse numérique des méthodes d'éléments finis hybrides et mixtes.* PhD thesis, Université Pierre et Marie Curie Paris, 1977
28. Wang, J., Mathew, T.P.: Mixed finite element method over quadrilaterals Conference on Advances In: *Numerical Methods and Applications* Dimov I.T. and Sendov B. and Vassilevski P. (Eds.), World Scientific, River Edge NJ 1994 pp 203–214
29. Wheeler, M.F., Yotov, I.: Multigrid on the interface for mortar mixed finite element methods for elliptic problems. *Comput. Meth. Appl. Mech. Eng.* **184**, 287–302 (2000)
30. Wohlmuth, B.I.: A mortar finite element method using dual spaces for the Lagrange multiplier. *SIAM J. Numer Anal* **38**(3), 989–1012 (2000)
31. Yotov, I.: Mixed finite element methods for flow in porous media. Rice University 1996 Houston Texas TR96-09 Dept. Comp. Appl. Math. Rice University and TICAM report 96-23 University of Texas at Austin